Trion dynamics in lead halide perovskite nanocrystals (EP)

Yoshihiko Kanemitsu[a] (ID)

AFFILIATIONS

Institute for Chemical Research, Kyoto University Uji, Kyoto 611-0011, Japan

Note: The paper is part of the JCP Special Topic on Lead Halide Perovskites.
[a]Author to whom correspondence should be addressed: kanemitu@scl.kyoto-u.ac.jp

ABSTRACT

Metal halide perovskite semiconductors fabricated with simple low-temperature solution processes are a unique class of materials anticipated for use in photonic devices such as solar cells, light-emitting diodes, and light modulators. The metal halide perovskites in the form of nanocrystals are particularly attracting attention as novel functional materials because of their exceptionally high luminescence efficiencies and wide range of possible luminescence wavelengths. By combining different optical characterization techniques, that is, single-dot spectroscopy, photon correlation spectroscopy, femtosecond transient absorption spectroscopy, and time-resolved photoluminescence spectroscopy, we study the dynamics of excitons, trions, and biexcitons in perovskite nanocrystals. Here, we provide a concise review of recent developments in this research field with a focus on trions in lead halide perovskite nanocrystals. A deep understanding of trion dynamics is especially important because they determine the luminescence properties of nanocrystals and are related to the ionization processes of nanocrystals.

Published under license by AIP Publishing. https://doi.org/10.1063/1.5125628

I. INTRODUCTION

For almost 40 years, semiconductor nanocrystals (NCs) have constituted the central material of nanoscience and have been widely investigated.[1–12] Among their various useful properties, the optical properties that depend on the NC size have opened up avenues for basic research and novel applications in many fields. The quantum confinement of excitons (electron–hole pairs) in NCs is responsible for many fascinating optical phenomena that cannot be observed in bulk crystals. As an example, NCs made from indirect-gap Si,[13–15] Ge,[16] and SiC[17] semiconductor materials show highly efficient luminescence even at room temperature, despite that their bulk counterparts exhibit only poor luminescence. This evidences that outstanding functional properties can be readily obtained with NCs. With the development of high-quality colloidal NCs, which can be fabricated without the need of expensive ultrahigh vacuum facilities like those required for molecular beam epitaxy, many researchers in different fields were able to get involved in the NC research. By the early 1990s, it had become possible to obtain stable photoluminescence (PL) as a result of the

development of high-quality NCs with high luminescence efficiencies and uniform size (e.g., CdSe NCs[18] and core/shell NCs[19–21]). Owing to this technological advance, the use of NCs was proposed for many applications.

The understanding of the optical properties of NCs significantly advanced through both improvements in sample fabrication technologies[18–25] including core/shell-type NC synthesis and precise characterization by modern laser spectroscopy (such as single-dot spectroscopy and femtosecond pump–probe spectroscopy).[26–29] From a viewpoint of fundamental physics, NCs are especially useful because the excited electrons inside the NC can be individually counted in contrast to bulk crystals. Therefore, the detailed discussion of exciton-related optical phenomena becomes possible. Moreover, the effect of quantum confinement and reduced dielectric constants in NCs enhances the Coulomb interactions, leading to novel multiple-exciton processes such as quantized Auger recombination[30–36] and multiple exciton generation.[37–44] A wide range of optical responses of NCs are determined by excited states such as a single exciton, a trion (charged exciton) formed by one exciton and a bound electron or hole, a biexciton which comprises two
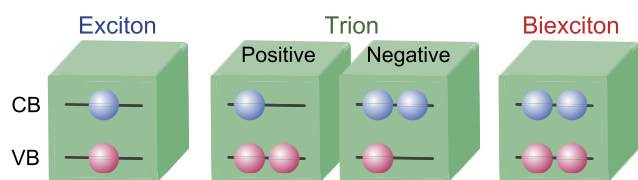
FIG. 1. Illustration of exciton, positive trion, negative trion, and biexciton in single NCs. These exciton complexes are different excited states with electrons in the conduction band (CB) and holes in the valence band (VB).

electrons and two holes, and other many-particle states. Figure 1 depicts four NCs containing different numbers of excited electrons in the conduction band (CB) and holes in the valence band (VB). The nonradiative Auger recombination of trions and biexcitons usually determines the NC's PL quantum yield (PLQY) and PL lifetime[45–48] and also induces unique phenomena such as PL intermittency.[49–55] As their deep understanding is extremely important for efficiency improvements of NC-based photonic devices such as solar cells and light-emitting diodes, there have been extensive studies on the PL intermittency mechanisms and recombination dynamics of trions and biexcitons.

In addition to the covalent semiconductors such as CdSe and PbSe, which have been investigated in detail so far, recently, the halide perovskite ionic semiconductors have been attracting much attention. It is becoming more and more evident that bulk optical properties of halide perovskites largely differ from those of conventional semiconductors like GaAs and CdSe.[56–60] The perovskite NCs, which can be fabricated by a simple colloidal synthesis, inherit the excellent optical properties of the perovskite bulk crystals and also exhibit novel photophysics induced by quantum confinement effects. As such, they are highly anticipated functional materials for photonics.[61,62]

In this review, we summarize recent results regarding the room-temperature luminescence properties of lead halide perovskite NCs. The recombination dynamics of excitons, trions, and biexcitons in lead halide perovskite NCs are studied by performing single-dot PL spectroscopy and femtosecond time-resolved spectroscopy of ensemble NCs. We discuss the trion generation and recombination dynamics and the ionization mechanisms of halide perovskite NCs.

II. LEAD HALIDE PEROVSKITE SEMICONDUCTORS

A. Electronic structure and luminescence properties of bulk crystals

The different types of lead halide perovskites can be represented using their chemical composition $APbX_3$. As shown in Fig. 2(a), the lead halide perovskite crystal contains robust inorganic octahedra (composed of lead and halogen atoms) and the A-site cation between them. The fundamental optical and electrical properties are mainly determined by the inorganic octahedron, PbX_6. By using I, Br, or Cl in the X site, the bandgap energy can be continuously changed within a wide wavelength range extending from the near infrared to the blue.[60] For the A-site cations, organic molecules, such as $CH_3NH_3^+$ (MA), $CH(NH_2)_2^+$ (FA), or inorganic ions like Cs^+ can be used. By using mixtures of different cations in the A site and different halogens in the X site, the photovoltaic characteristics and durability of solar cell devices can be strongly improved.[63] One characteristic of halide perovskites is that their compositions can be easily controlled by using simple chemical techniques. This enables easy fabrication of materials with various different functionalities.

An important aspect for photonic device applications is that the lead halide perovskite semiconductors have direct band-to-band transitions.[64] The conduction band reflects the p orbital of the Pb atom, and as shown in Fig. 2(b), it consists of the heavy electron (he), the light electron (le), and, furthermore, a separated spin split-off (so) band due to spin–orbit interaction.[64,65] Since the orbital degeneracy at the conduction-band edge is small, more than two excitons cannot be generated in the lowest excited state if the crystal size is reduced to about several nanometers (therefore, analysis of exciton relaxation in lead halide perovskite NCs is relatively easy).[66] Both the bottom of the conduction band and the top of the valence band of a lead halide perovskite semiconductor are formed from antibonding orbitals. Owing to this characteristic, deep lying defect

(a)

(b)
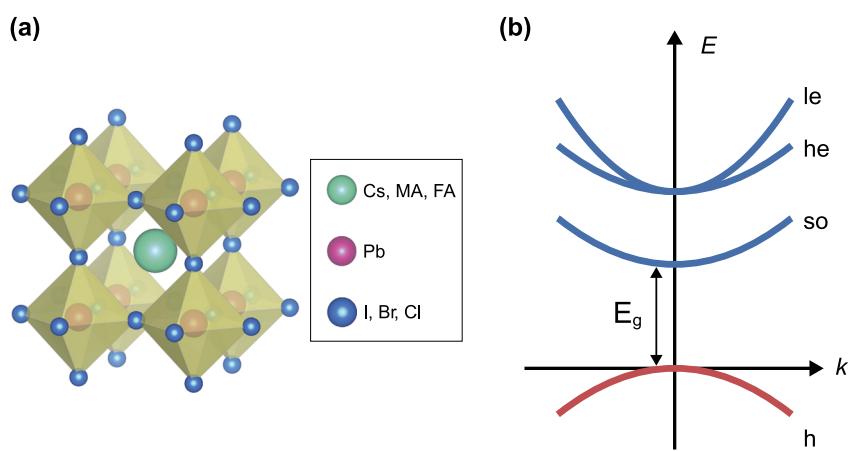
FIG. 2. (a) Cubic structure of $APbX_3$ lead halide perovskite crystals. (b) Schematic of electronic band structure of lead halide perovskites near the band edge. E_g is the bandgap energy.

levels hardly form within the bandgap.[67] Furthermore, the refractive index of a perovskite semiconductor decreases with increasing temperature.[68] This effect is opposite to the characteristic of common inorganic semiconductors such as Si and GaAs and thus can be utilized to compensate temperature drifts of inorganic optical devices.[68]

Although halide perovskites are semiconductors that can be fabricated by solution processes, they are semiconductors with exceptionally low densities of defects and exhibit highly efficient PL. When focusing on data obtained from MAPbX$_3$, we can list down optical characteristics such as (1) a sharp absorption edge reflecting low densities of localized levels within the bandgap, (2) an internal luminescence efficiency that approaches 100% even at room temperature, (3) free-carrier band-to-band emission and free-exciton emission, (4) efficient photon recycling, and (5) anti-Stokes PL due to strong electron–phonon interactions.[69–77] These properties, which are advantageous for solar cells in particular and also light-emitting diodes and lasers, and the cost-effective fabrication of perovskite layers with high quality are the reasons for the huge popularity of this material system.

B. Synthesis and optical properties of NCs

The first synthesis of perovskite NCs was reported for the organic–inorganic hybrid MAPbBr$_3$ perovskite NCs in the year 2014.[78] However, at that time, the large nonuniformity of the NC sizes and a low PLQY of about 20% remained issues to be solved. Owing to the first successful fabrication of stable all-inorganic CsPbX$_3$ (X = Cl, Br, I) perovskite NCs, it was possible to start the NC research at full scale by 2015.[79] By the synthesis of CsPbX$_3$ NCs through the hot injection method and exchange of the halogen atom, luminescence colors extending over the whole visible regime have been obtained.[80] CsPbX$_3$ NCs exhibit high PLQYs of 50%–90% despite the simple synthesis method without any special surface treatment.[80] These high PLQY values can compete with those of core/shell CdSe/ZnS and CdSe/CdS NCs, which have to be synthesized by precise control of reaction time and temperature. Additionally, the CsPbX$_3$ NCs adopt the form of well-defined cubes and have a good size uniformity.[79]

The perovskite NCs possess a unique exciton structure as a result of the perovskite's band structure: the fine structure present in the energy states can be described by the optically allowed bright exciton and the optically forbidden dark exciton.[81] In CdSe NCs, which are well-studied NCs, the recombination path via the dark exciton becomes dominant at low temperatures, and thus, the PL lifetime becomes extremely long.[82,83] In contrast, it has been verified that at low temperatures, the CsPbX$_3$ NCs exhibit a very short PL lifetime of subnanoseconds.[81] It has been shown that the exciton triplet state in CsPbX$_3$ perovskite NCs has a lifetime that is much shorter than that of other inorganic or organic semiconductors and that it is optically active, i.e., bright.[81] Theoretical calculations for the CsPbX$_3$ NC including the Rashba effect predict that the energy level of this bright triplet exciton is below that of the singlet exciton. However, many single-dot spectroscopy measurements have been performed, and as there are also reports stating that the *dark* exciton state has the lowest energy, the clarification of the low-temperature exciton fine structure in perovskites is still being awaited.[84–90]

In case that multiple excitons exist in a NC, the interactions between the excitons become important. It has been shown that when the binding energy of a biexciton in a CsPbX$_3$ NC is determined from the difference between the PL peak energies of the biexciton and exciton states, a value three times larger than that for a CdSe NC is obtained.[91] Additionally, the Auger recombination rate in CsPbX$_3$ NCs is about ten times faster than that of CdSe and PbSe NCs with the same NC volume.[66,92] Based on these reports, it has been clarified that the Coulomb interaction between two excitons in a perovskite NC is strong.[93] This fact indicates that perovskite NCs are excellent materials for investigations of many-body effects of excitons. The large Coulomb interaction leads to a loss of biexcitons induced by fast Auger recombination, which is often considered detrimental.[34,36] However, the Auger recombination can be beneficial from the viewpoint of single-photon emitters because it inhibits multiple photon emission from multiple excitons.

III. RECOMBINATION DYNAMICS OF EXCITONS, TRIONS, AND BIEXCITONS

The PL properties of a NC depend strongly on the number of excitons generated inside the NC. The analysis method explained below allows us to quantify the dependences of PL intensities of excitons, trions, and biexcitons on the excitation fluence. In order to determine the average number of excitons generated in a NC upon excitation, $\langle N \rangle$, it is first necessary to measure the absorption cross section of the NC, σ. The average number of photons absorbed by a NC equals $\langle N \rangle$ and can be expressed by the product of σ and the excitation photon flux per unit area, j_{ex}. For the distribution of the number of excitons generated in NCs, we assume the Poisson distribution.[34] This distribution together with the fact that at least one photon has to be absorbed by a single NC to generate one exciton allows us to derive an analytical expression for the excitation fluence dependence. When we denote the exciton PLQY by η_X, the excitation power dependence of the exciton PL intensity I_X is given by the following equation:

$$I_X = \eta_X \left(1 - e^{-\langle N \rangle}\right) = \eta_X \left(1 - e^{-j_{ex}\sigma}\right). \quad (1)$$
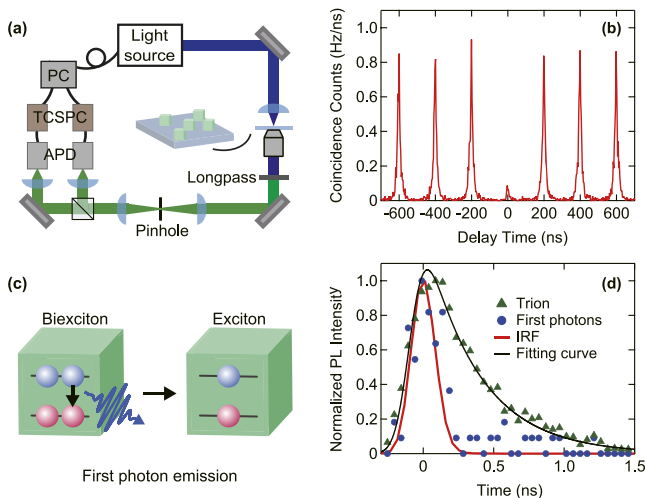
By employing Eq. (1), we can determine the NC's absorption cross section from the dependence of the exciton PL intensity with respect to the excitation photon flux. We note that the absorption cross section can be also determined from the excitation fluence dependence of transient absorption (TA) signals.[34,94] Furthermore, the excitation fluence dependence of the biexciton PL intensity, I_{XX}, can be described in a similar way,

$$I_{XX} = \eta_{XX} \left(1 - e^{-\langle N \rangle} - \langle N \rangle e^{-\langle N \rangle}\right) = \eta_{XX} \left(1 - e^{-j_{ex}\sigma} - j_{ex}\sigma e^{-j_{ex}\sigma}\right). \quad (2)$$
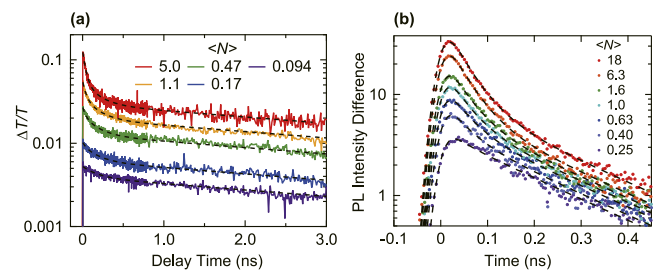
Here, η_{XX} is the PLQY of the biexciton. An important point is that subsequent emission of two photons is possible for the biexciton. This process is called two-photon cascade emission,[95–98] and it can be clarified through single-dot spectroscopy.

In order to determine η_{XX}, it is necessary to measure the second-order photon correlation function $g^{(2)}(t)$ as a function of time t by a Hanbury Brown–Twiss interferometer as shown in

Fig. 3(a). The pulsed light source excites the diluted NC ensemble on a transparent substrate, and the PL signal of a single NC is measured by a pair of avalanche photodiodes (APDs). Their responses are recorded by a time-correlated single photon counting (TCSPC) board. The $g^{(2)}(t)$ data correspond to the occurrences when both APDs detect a photon within a given delay time. An example for the $g^{(2)}(t)$ of the PL from a single CsPbBr$_3$ NC that is excited by a pulsed laser with a repetition frequency of $1/t_{rep} = 5$ MHz is shown in Fig. 3(b).[94] The average size of NCs in this ensemble on the transparent substrate is 7.7 ± 1.1 nm, and the data are obtained for $\langle N \rangle \sim 0.07$. We can confirm that peaks appear corresponding to the repetition frequency of the excitation pulses. The side peaks are large and have almost the same integrated counting rate g_s. The important point is the center peak at $t = 0$; here, the two detectors simultaneously detect photons with a nonzero rate g_c, indicating that two individual photons were emitted by the NC. This indicates the existence of a two-photon cascade emission from a biexciton, as shown in Fig. 3(c). The lifetime of the first photon emission in the cascade process is shown in Fig. 3(d), which clarifies that the lifetime of the biexciton is faster than the measurement limit of 200 ps for this single-dot spectroscopy setup. In the weak excitation regime $\langle N \rangle \ll 1$, the quantum efficiency of the two-photon cascade emission, η_{XX}/η_X, becomes equal to g_c/g_s, and thus, it can be easily determined by measuring $g^{(2)}(t)$ only.[95,96] If we simultaneously perform the measurements of the PL decay curves in addition to $g^{(2)}(t)$, we can actually measure g_c/g_s and I_{XX}/I_X for a wide range of excitation fluences.[98,99] This approach constitutes a

FIG. 4. (a) Excitation fluence dependence of the TA decay curves monitored at the CsPbBr$_3$ NC exciton ground state energy. The excitation fluence is expressed in terms of average absorbed photons per NC. The decay curves are fitted using triple exponential functions (dashed curves). (b) Fast decay components of the PL curves as a function of the excitation fluence. The resulting curves are fitted using double exponential functions. Figures are adapted with permission from Yarita et al., J. Phys. Chem. Lett. **8**, 1413 (2017). Copyright 2017 American Chemical Society.

measurement method of wide applicability.[98,99] In this way, single-dot spectroscopy is extremely powerful, as only this measurement enables us to clearly distinguish between exciton and biexciton PL properties.

In order to characterize the fast biexciton and trion recombination time constants with higher time-resolution, we can employ femtosecond TA spectroscopy measurements of NC ensemble samples. Figure 4(a) shows the excitation fluence dependence of the time evolution of the ground-state exciton population in the CsPbBr$_3$ NCs.[94] For the weak excitation condition $\langle N \rangle = 0.094$, the TA decay curve consists of a single exponential component which shows that the exciton has a recombination time constant on the order of nanoseconds. On the other hand, as the excitation fluence is increased, faster decay components clearly appear. The two faster lifetimes are obtained by fitting with a triple exponential function. Time-resolved PL spectroscopy also allows us to observe the three components in a similar way. As the slow PL component is that of the exciton, we plot the fast components obtained by subtracting this slow component from the actually measured PL decay data in Fig. 4(b). The single-dot and ensemble-averaged optical measurements clarify that the biexciton lifetime is about 40 ps and that of the trion is about 200 ps.

We note that the combination of microscopic spectroscopy of a single NC and TA measurements (performed on the NC ensemble sample) enables us to clarify the recombination dynamics of excitons, trions, and biexcitons in perovskite NCs because their recombination lifetimes are extremely short compared with other conventional semiconductor NCs.
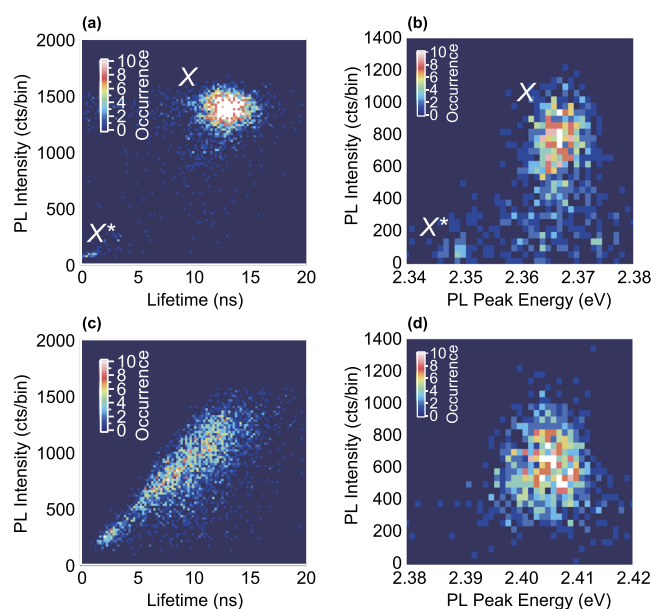
IV. IMPACT OF SURFACE TRAP STATES ON THE EXCITON DYNAMICS

To discuss the intrinsic optical properties of semiconductor NCs, the single-dot spectroscopy proves to be useful because individual NCs with different optical responses can be examined. In the following, we present some experimental results on trion dynamics in organic–inorganic halide perovskite NCs. It is known that the

FIG. 3. (a) Experimental setup to measure the second-order photon correlation function $g^{(2)}$. The PL signals of a single NC are measured by a pair of avalanche photodiodes (APDs) connected to a time-correlated single photon counting (TCSPC) board. (b) $g^{(2)}$ data obtained from a single CsPbBr$_3$ NC. (c) Illustration of the first photon emission and (d) PL dynamics of a trion and a biexciton. The latter is characterized via the first photon emission in the cascaded emission. The instrumental response function (IRF) of the measurement system is shown with the red solid curve. Figures (b) and (d) are adapted with permission from Yarita et al., J. Phys. Chem. Lett. **8**, 1413 (2017). Copyright 2017 American Chemical Society.

degradation of perovskite NC samples occurs under strong light illumination in air. A significant blueshift of the PL peak energy and a decrease in the PL intensity are observed during sample degradation.[100,101] However, in our measurements presented in this paper, the blueshift of the PL peak and the decrease in the PL intensity are not observed.

A representative example of the temporal change in the PL intensity of a single FAPbBr$_3$ NC during light illumination is shown in Fig. 5.[102] Among the total of 67 NCs that have been measured, 37 NCs exhibit a PL blinking which can be characterized by two discrete states, i.e., the on state with a high PL intensity (the intensity region shown in red) and a state with low PL intensity (the intensity region shown in blue) [Fig. 5(a)]. On the other hand, the remaining 30 NCs exhibit a flickering behavior, that is, the PL intensity changes more gradually [Fig. 5(b)]. Note that during these measurements, a blueshift of the PL peak and a decrease in the PL intensity has not been observed,[102] and we also conclude that the degradation of NCs is not the origin of the flickering behavior.
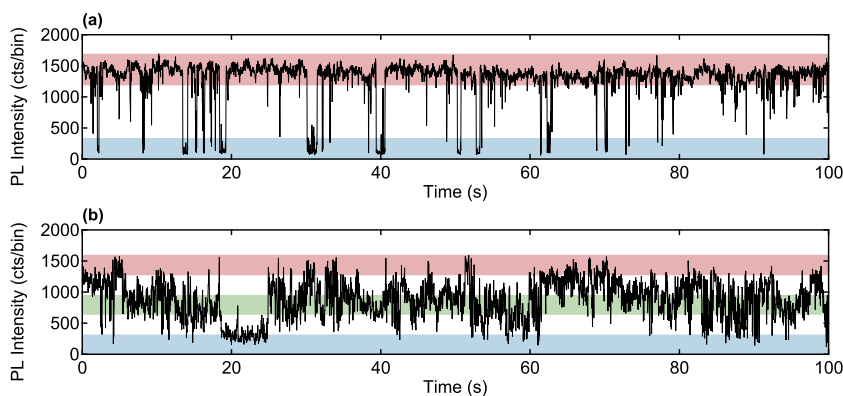
Figure 6 summarizes the correlations between the PL peak energies, PL lifetimes, and the PL intensities of the blinking and flickering NCs.[102] For the blinking NC, we can confirm PL from two excited states: the exciton (X) with its characteristic high PL intensity and long lifetime, and the positively charged trion (X^+) with a low PL intensity and a short lifetime [Fig. 6(a)] (the latter assignment is based on experiments with surface treatments as explained below). These two states can also be observed in the correlation between PL intensity and PL peak energy [Fig. 6(b)]. On the other hand, for the flickering NC, the PL intensity, lifetime, and also the PL peak energy only fluctuate relatively largely [Figs. 6(c) and 6(d)]. We note that these relations are also affected by the size dependence of the PL lifetime, which is explained in the following. As shown in Fig. 7(a), the PL that exhibits a clear dependence on the size (absorption cross section) is that from the exciton[102] because the state with the large PL intensity is the state with the long lifetime. This size dependence is independent of the type of PL intermittency. On the other hand, for the state with short PL lifetime, there is a large difference between the size dependences of blinking and flickering types [Fig. 7(b)]. In the NCs that exhibit blinking, the fast decay component shows a clear size dependence (dashed line for blinking NCs) since it is caused by biexcitons or trions. In contrast, no

size dependence is observed for the fast component of the flickering NCs. This suggests that flickering is a phenomenon that originates from extrinsic factors such as surface states and surrounding environment.

Evidence for this interpretation can be obtained by modifying the surfaces of FAPbBr$_3$ NCs by sodium thiocyanate (NaSCN).[103] After the surface modification, almost no NC exhibits flickering and the PLQY of the FAPbBr$_3$ NCs significantly improves. Furthermore, the absorption cross section of surface-modified FAPbBr$_3$ NCs exhibits a clear dependence with respect to the integrated PL intensity.[102] With these results, it has been clarified

FIG. 6. Correlation between (a) PL intensity and PL lifetime and (b) PL intensity and PL peak energy for a blinking NC. [(c) and (d)] The corresponding correlations for a flickering NC. Figures are adapted with permission from Yarita et al., J. Phys. Chem. Lett. 8, 6041 (2017). Copyright 2017 American Chemical Society.

FIG. 5. PL intensity time trace of (a) a blinking FAPbBr$_3$ NC and (b) a flickering FAPbBr$_3$ NC. Figures are adapted with permission from Yarita et al., J. Phys. Chem. Lett. 8, 6041 (2017). Copyright 2017 American Chemical Society.
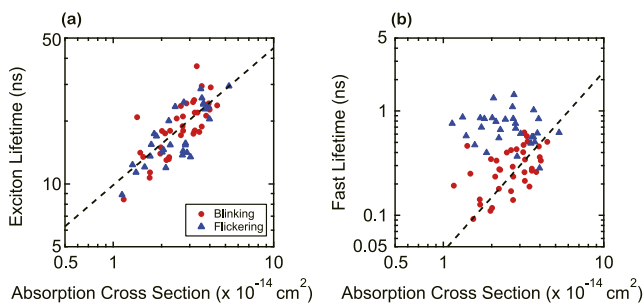
FIG. 7. Summary of (a) the exciton lifetimes and (b) the fast decay lifetimes as a function of the absorption cross sections of 67 different NCs exhibiting either blinking or flickering. Figures are adapted with permission from Yarita et al., J. Phys. Chem. Lett. **8**, 6041 (2017). Copyright 2017 American Chemical Society.

FIG. 8. (a) Formation of a negatively ionized NC by photochemical doping. A reducing agent is used to extract the photogenerated hole from the NC, leaving behind an excess electron in the CB of the NC. (b) Formation of a negatively ionized NC by Auger ionization after a biexciton has been generated in the NC. Photoexcitation of these NCs leads to negatively charged excitons or so-called negative trions.
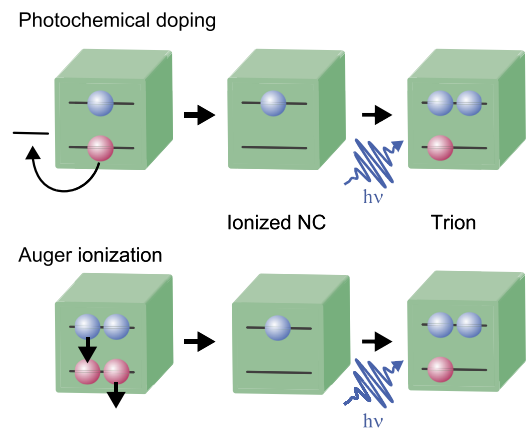
that the flickering can be controlled by the surface modification with NaSCN, and the reason for this is the electron supply to trap levels that exist on the NC surface.[103] Although defects cannot be easily formed in lead halide perovskites,[67] a NC PLQY close to 100% requires the precise control of the surface states.[103–105]

V. POSITIVE AND NEGATIVE TRIONS IN PEROVSKITE NANOCRYSTALS

We have mentioned that trions are formed in perovskite NCs and that their recombination dynamics govern the PL properties. As shown in Fig. 1, the trion is a three-particle state and two configurations are possible: the positively and the negatively charged states. The trion generation process is related to the ionization of the NC, and the following two processes have to be considered: First, by chemical treatment of the NC surface, it is possible to extract a photogenerated hole from the inside of the NC, and an ionized NC can be obtained [Fig. 8(a)].[106,107] Second, an ionized NC is generated by Auger recombination of a biexciton and a trion state appears upon subsequent photoexcitation [Fig. 8(b)]. The same process has also been reported for carbon nanotubes; the trion generation is possible by chemical doping as well as optical doping.[108–110]

Here, we discuss the photophysics of trions in a NC thin film that is doped with a material that can extract photoexcited holes from the NCs.[111] The NCs in the film exhibit blinking behavior and thus allow us to clearly observe the contribution of trions in the PL signal. In Fig. 9(a), we show the PL intensity time trace of an as-prepared single FAPbBr$_3$ NC (average edge length is about 10.5 nm), which has not been chemically treated after fabrication.[111] We can clearly observe the abrupt transitions between the state with high PL intensity (region indicated with red) and the state with low PL intensity (region indicated with blue). The existence of these two states can be also inferred by drawing the event histogram as shown in the right-hand side of Fig. 9.

By adding copper thiocyanate (CuSCN)[112] to the FAPbBr$_3$ NC thin film, the PL blinking behavior strongly changes: the occupation probability of the state with the low PL intensity becomes almost zero, and instead a new intermediate state appears [Fig. 9(b)]. In

order to investigate the origins of the three different states with high, intermediate, and low PL intensities, we separately measured the PL dynamics for each state in the single FAPbBr$_3$ NCs by time-tagged single photon detection.[98] The state with the high PL intensity exhibits a single exponential decay with a long lifetime of 21 ns [Fig. 10(a)]. The lifetime of this state is about 20 ns on average for both NCs with and without CuSCN additive. Therefore, this state is assigned to the neutral NC containing one exciton. We emphasize that the PL lifetime of a single NC changes according to the size of the monitored NC. The average lifetimes obtained in this experiment are equal to the lifetime of the neutral exciton obtained from an ensemble of NCs dispersed in hexane.

In the PL decay curve of the intermediate state, a fast lifetime component (600 ps) appears as shown in Fig. 10(b). As CuSCN is a material that enables extraction of a photoexcited hole from a perovskite NC, this component is assigned to the Auger recombination of the negative trion. The lifetime of the state with low PL intensity shown in Fig. 10(c) is significantly faster (330 ps). Because the intentional negative ionization of the NC by CuSCN leads to suppression of the state with low PL intensity, this short lifetime is assigned to the Auger recombination of the positive trion.

In order to verify the above assignment, we investigated the relation between the biexciton lifetime, the lifetime of the negative trion, τ_{X-}, and the lifetime of the positive trion, τ_{X+}. We can express the biexciton lifetime τ_{XX} in terms of the lifetimes of the trions,[48]

$$\tau_{XX}^{-1} = 2\left(\tau_{X-}^{-1} + \tau_{X+}^{-1}\right). \quad (3)$$

The distribution of the predicted biexciton lifetimes for the 67 NCs is shown in the histogram in Fig. 10(d) and the average value is about 100 ps. To obtain an exact value for such
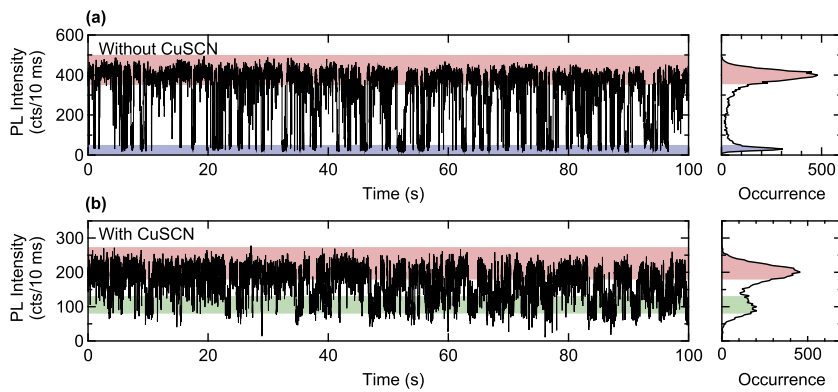
FIG. 9. PL intensity time trace for a single FAPbBr₃ NC in (a) a thin film without CuSCN and (b) a thin film with CuSCN. The right-hand side of (a) and (b) represents the event histogram. Figures are adapted from Yarita *et al.*, Phys. Rev. Mater. **2**, 116003 (2018). Copyright 2018 Author(s), licensed under a Creative Commons Attribution 4.0 License.

a short biexciton lifetime, we performed femtosecond TA spectroscopy of FAPbBr₃ NCs dispersed in hexane.[111] The result is shown with the red arrow. It is found that this lifetime well agrees with the predicted average value calculated from the sets of negative and positive trion lifetimes of each NC. This result supports the assignments of states with intermediate and low PL intensities to NCs containing negative and positive trions, respectively.
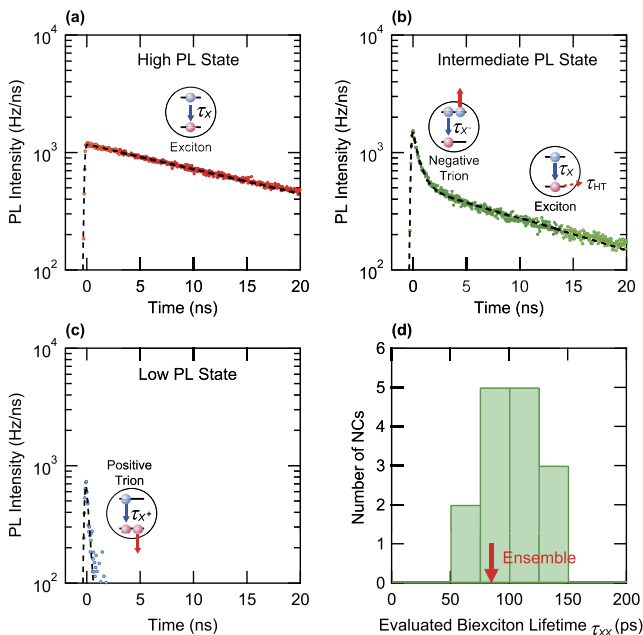
FIG. 10. PL decay curves derived from the time-tagged time-resolved PL data for the states with (a) high PL intensity, (b) intermediate PL intensity, and (c) low PL intensity. (d) Histogram of the biexciton Auger lifetime predicted from the experimentally determined lifetimes of negative and positive trions. The red arrow indicates the actual biexciton Auger lifetime measured by TA spectroscopy of an ensemble of NCs. Figures are adapted from Yarita *et al.*, Phys. Rev. Mater. **2**, 116003 (2018). Copyright 2018 Author(s), licensed under a Creative Commons Attribution 4.0 License.

VI. TRIONS AND IONIZATION OF NANOCRYSTALS

The trion in the NC is frequently in the focus of interest because it is directly related to the ionization of the NC. In case that electron or hole traps exist on the NC surface, it can be considered that these traps play an important role in the ionization of the NC's interior and trion generation. Furthermore, it is known that the photoionization of NCs depends strongly on the measurement conditions such as stirring of the sample.[113] To clarify further details, we prepared CsPbBr₃ NCs with and without surface treatment by NaSCN and performed femtosecond TA spectroscopy measurements of each sample under static and stirred conditions. This enables studying the ionization of NCs via the trion generation yield.[114]

As mentioned in Sec. III, while an almost single exponential decay is present due to the exciton in the NC under weak excitation conditions, faster decay components appear due to trions and biexcitons as the excitation fluence increases. In order to compare the degrees of trion generation under the above-mentioned four measurement conditions, we consider the ratio of trion TA amplitude to exciton TA amplitude, A_{X*}/A_X. The plot of this ratio as a function of the average number of photons absorbed by a NC is shown in Fig. 11. It is found that the extent of the trion generation can be suppressed by both stirring and surface treatment.[114]

To investigate the ionization of NCs, two trion generation processes are considered: the generation from an ionized NC and the generation from a neutral NC. In order to generate a trion in an ionized NC, it is sufficient to generate one electron–hole pair [Fig. 8(a)]. In the case of the neutral NC, the generation of an excess carrier via a nonradiative process between at least two electron–hole pairs has to be involved [Fig. 8(b)]. According to this model, we can derive the ratio of trion signal to exciton signal by using Eqs. (1) and (2),

$$\frac{A_{X*}}{A_X} = a + \frac{b\left(1 - e^{-\langle N \rangle} - \langle N \rangle e^{-\langle N \rangle}\right)}{1 - e^{-\langle N \rangle}}. \tag{4}$$
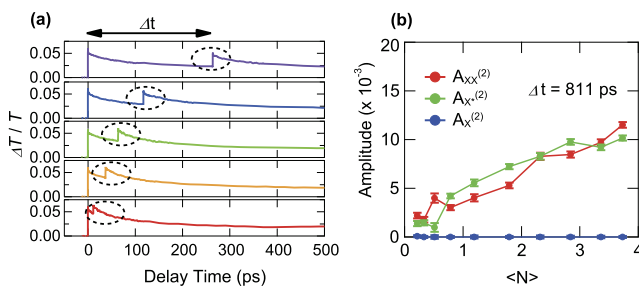
The fitting results obtained by using this equation are shown with the solid curves in Fig. 11. We can confirm that this model allows us to reproduce the experimental results. From the present analysis, we can infer that the dominant trion generation process under weak
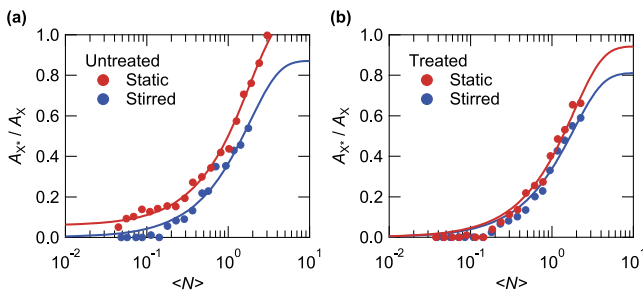
FIG. 11. (a) Excitation fluence dependence of ratio between the trion and exciton TA amplitudes for the untreated CsPbBr$_3$ NCs. The red and blue circles represent the results estimated by triple-exponential fitting of the TA data. (b) Results for the surface-treated NCs. The solid curves show the fitting results using Eq. (4). Figures are adapted with permission from Nakahara et al., J. Phys. Chem. C, **122**, 22188 (2018). Copyright 2018 American Chemical Society.

excitation is the one involving the ionized NC, and this process can be suppressed by stirring and also surface treatment. Under strong excitation conditions, the trion generation starting from neutral NCs becomes dominant, and this process involves the nonradiative Auger recombination of biexcitons.

To confirm the existence of ionized NCs induced by strong photoexcitation, TA experiments that employ two successive pump pulses with a tunable pump delay time Δt are useful.[115] To ionize many of the NCs in the ensemble, the first pump pulse illuminates the NCs (stirred but not surface treated) with a strong excitation intensity that corresponds to $\langle N \rangle = 5.1$. Under this condition, $\geq 99\%$ of the NCs absorb at least one photon and $\geq 95\%$ absorb more than one photon. Therefore, biexcitons or trions are generated in almost all NCs by the first pump pulse. By changing the delay of the second pump pulse, we obtain different TA signals as shown in Fig. 12(a). For a pump delay time $\Delta t = 811$ ps, almost all biexcitons and trions have recombined but excitons still exist due to their long lifetime. Therefore, the second pump pulse mainly excites NCs containing either one exciton or a single excited carrier (ionized NCs). In other words, it is expected that only components of biexcitons and trions appear in response to the second pump. By subtracting the TA signal that is obtained by single-pulse excitation from the TA signal in the above outlined double-pump scheme, the effect of the ionized NCs can be extracted. The TA amplitudes of the different components can be obtained from the analysis of the decay of this difference TA signal.[115] The actual biexciton, trion, and exciton TA amplitudes induced by the second pump pulse for $\Delta t = 811$ ps are summarized in Fig. 12(b). NCs containing trions and biexcitons are generated by the second pulse, while almost no additional NCs with single excitons are generated. The result evidences that NC ionization via the nonradiative Auger recombination of biexcitons occurs. Moreover, from the rate equations, we are able to evaluate the ionization probabilities of NCs that contain a trion or a biexciton. We find that the NC ionization rate involving trions is larger than that involving biexcitons.[115] This is reasonable because both radiative and nonradiative Auger recombination processes of trions contribute to the generation of ionized NCs.

VII. CONCLUSIONS AND PERSPECTIVES

We provided a concise summary of the behaviors of excitons, trions, and biexcitons in lead halide perovskite NCs at room temperature. We explained that their behaviors can be clarified by combining single-dot spectroscopy and femtosecond TA spectroscopy. The nonradiative Auger recombination processes of trions and biexcitons induce a reduction in the PL efficiency, lifetime, and intermittency. The generation and recombination dynamics of trions are especially important from the viewpoint of device performance. Their influences can be verified, for example, in previous reports on efficiency improvements of light-emitting diodes by suppression of trion generation.[116] By chemical treatment of the NC surface and surrounding environment, the formation of positive and negative trions can be manipulated. Their Auger recombination lifetimes are different from each other. Experimental studies on the relation between the NC surface condition that has been chemically modified and the resulting PL dynamics help us to understand the intrinsic optical properties of perovskite crystals.

The detailed studies of the energy structures of excitons and trions are also useful for the identification of the interior crystalline structure and the surface localized structure of individual NCs. At cryogenic temperatures, the PL linewidth of excitons and trions becomes very narrow and the recombination dynamics of the trions can be studied by single-dot PL measurements.[84,85,89] The PL spectrum and dynamics can be discussed in conjunction with complexed exciton fine structures. The low-temperature single dot spectroscopy will clarify the dynamics of excitons and trions and the fine structure of electronic states in more detail. Even at room temperature, perovskite NCs shows narrow PL linewidths because of weak and moderate quantum confinement of carriers in relatively large-sized NCs. Because of large oscillator strengths of halide perovskites,[81,117] their exciton PL decay rates are large compared to those of conventional metal-chalcogenide NCs. Moreover, it has been recently reported that highly monodispersed cubic NCs can form micrometer-sized cubic crystals by self-assembly and they show unique light emission.[118] Cubic perovskite NCs with these outstanding PL properties will open up new

FIG. 12. Double-pump TA spectroscopy of CsPbBr$_3$ NCs. (a) Dependence of the TA decay curves on the pump delay time Δt. (b) TA amplitudes of excitons, trions, and biexcitons generated by the second pump (impinging at $\Delta t = 811$ ps) as a function of the excitation fluence of the second pump pulse. Figures are adapted with permission from Nakahara et al., J. Phys. Chem. Lett. **10**, 4731 (2019). Copyright 2019 American Chemical Society.

opportunities for fundamental optics as well as photonic device applications.

The understanding of the trion generation dynamics is important for the understanding of ionization mechanisms of NCs. Ionized NCs provide a unique experimental stage to study single-carrier spin and/or transport properties by selective doping of an electron or a hole within NCs. In addition, since the Auger lifetime of trions is much longer than that of biexcitons, ionized NCs show long gain lifetimes. Long-lived trions can reduce the threshold for optical gains and cause the efficient amplified spontaneous emission.[119,120] Moreover, we anticipate that positively or negative ionized NCs becomes a unique class of materials for electrical transport, selective photochemical reactions, light-emitting devices, and so on. We believe that suppression or increase in trion generation is necessary to develop novel functions of NCs.

The research field of environmentally friendly lead-free perovskites and related compounds has become active during the last five years.[121] In particular, unique zero-dimensional (0D) halide materials and double-perovskite halide materials were synthesized for light-emitting materials.[122–125] They show very broadband white-light emission that originates from self-trapped excitons due to strong exciton-phonon coupling,[122–125] while the lead halide perovskite NCs show very narrow-band PL (high color purity) mentioned above. It is anticipated that the halide perovskite NCs and related halide compounds have great potential for the next-generation lighting and display technologies.

ACKNOWLEDGMENTS

REFERENCES

[1] A. I. Ekimov and A. A. Onushchenko, JETP Lett. **34**, 345 (1981).

[2] A. Henglein, Ber. Bunsen-Ges. Phys. Chem. **86**, 301 (1982).

[3] Al. L. Efros and A. L. Efros, Sov. Phys. Semicond. **16**, 772 (1982).

[4] L. E. Brus, J. Chem. Phys. **79**, 5566 (1983).

[5] A. I. Ekimov, Al. L. Efros, and A. A. Onushchenko, Solid State Commun. **56**, 921 (1985).

[6] L. Brus, J. Chem. Phys. **90**, 2555 (1986).

[7] Y. Kanemitsu, Phys. Rep. **263**, 1 (1995).

[8] A. P. Alivisatos, J. Phys. Chem. **100**, 13226 (1996).

[9] A. G. Cullis, L. T. Canham, and P. D. J. Calcott, J. Appl. Phys. **82**, 909 (1997).

[10] S. A. Empedocles, R. Neuhauser, K. Shimizu, and M. G. Bawendi, Adv. Mater. **11**, 1243 (1999).

[11] V. I. Klimov, J. Phys. Chem. B **110**, 16827 (2006).

[12] D. J. Norris, Al. L. Efros, and S. C. Erwin, Science **319**, 1776 (2008).

[13] L. T. Canham, Appl. Phys. Lett. **57**, 1046 (1990).

[14] Y. Kanemitsu, T. Ogawa, K. Shiraishi, and K. Takeda, Phys. Rev. B **48**, 4883 (1993).

[15] W. L. Wilson, P. F. Szajowski, and L. E. Brus, Science **262**, 1242 (1993).

[16] Y. Maeda, N. Tsukamoto, Y. Yazawa, Y. Kanemitsu, and Y. Masumoto, Appl. Phys. Lett. **59**, 3168 (1991).

[17] T. Matsumoto, J. Takahashi, T. Tamaki, T. Futagi, H. Mimura, and Y. Kanemitsu, Appl. Phys. Lett. **64**, 226 (1994).

[18] C. B. Murray, D. J. Norris, and M. G. Bawendi, J. Am. Chem. Soc. **115**, 8706 (1993).

[19] M. A. Hines and P. Guyot-Sionnest, J. Phys. Chem. **100**, 468 (1996).

[20] B. O. Dabbousi, J. Rodriguez-Viejo, F. V. Mikulec, J. R. Heine, H. Mattoussi, R. Ober, K. F. Jensen, and M. G. Bawendi, J. Phys. Chem. B **101**, 9463 (1997).

[21] X. Peng, M. C. Schlamp, A. V. Kadavanich, and A. P. Alivisatos, J. Am. Chem. Soc. **119**, 7019 (1997).

[22] Z. A. Peng and X. Peng, J. Am. Chem. Soc. **123**, 183 (2001).

[23] P. D. Cozzoli, T. Pellegrino, and L. Manna, Chem. Soc. Rev. **35**, 1195 (2006).

[24] D. V. Talapin, J.-S. Lee, M. V. Kovalenko, and E. V. Shevchenko, Chem. Rev. **110**, 389 (2010).

[25] M. Nasilowski, B. Mahler, E. Lhuillier, S. Ithurria, and B. Dubertret, Chem. Rev. **116**, 10934 (2016).

[26] A. J. Nozik, M. C. Beard, J. M. Luther, M. Law, R. J. Ellingson, and J. C. Johnson, Chem. Rev. **110**, 6873 (2010).

[27] J. Cui, A. P. Beyler, T. S. Bischof, M. W. B. Wilson, and M. G. Bawendi, Chem. Soc. Rev. **43**, 1287 (2014).

[28] M. J. Fernée, P. Tamarat, and B. Lounis, Chem. Soc. Rev. **43**, 1311 (2014).

[29] J. M. Pietryga, Y.-S. Park, J. Lim, A. F. Fidler, W. K. Bae, S. Brovelli, and V. I. Klimov, Chem. Rev. **116**, 10513 (2016).

[30] D. I. Chepic, Al. L. Efros, A. I. Ekimov, M. G. Ivanov, V. A. Kharchenko, I. A. Kudriavtsev, and T. V. Yazeva, J. Lumin. **47**, 113 (1990).

[31] I. Mihalcescu, J. C. Vial, A. Bsiesy, F. Muller, R. Romestain, E. Martin, C. Delerue, M. Lannoo, and G. Allan, Phys. Rev. B **51**, 17605 (1995).

[32] V. I. Klimov and D. W. McBranch, Phys. Rev. B **55**, 13173 (1997).

[33] V. I. Klimov, A. A. Mikhailovsky, D. W. McBranch, C. A. Leatherdale, and M. G. Bawendi, Science **287**, 1011 (2000).

[34] V. I. Klimov, Annu. Rev. Condens. Matter Phys. **5**, 285 (2014).

[35] V. I. Klimov, J. A. McGuire, R. D. Schaller, and V. I. Rupasov, Phys. Rev. B **77**, 195324 (2008).

[36] Y. Kanemitsu, Acc. Chem. Res. **46**, 1358 (2013).

[37] R. D. Schaller and V. I. Klimov, Phys. Rev. Lett. **92**, 186601 (2004).

[38] R. J. Ellingson, M. C. Beard, J. C. Johnson, P. Yu, O. I. Micic, A. J. Nozik, A. Shabaev, and Al. L. Efros, Nano Lett. **5**, 865 (2005).

[39] M. C. Beard, K. P. Knutsen, P. Yu, J. M. Luther, Q. Song, W. K. Metzger, R. J. Ellingson, and A. J. Nozik, Nano Lett. **7**, 2506 (2007).

[40] A. Ueda, K. Matsuda, T. Tayagaki, and Y. Kanemitsu, Appl. Phys. Lett. **92**, 233105 (2008).

[41] S. Wang, M. Khafizov, X. Tu, M. Zheng, and T. D. Krauss, Nano Lett. **10**, 2381 (2010).

[42] O. E. Semonin, J. M. Luther, S. Choi, H.-Y. Chen, J. Gao, A. J. Nozik, and M. C. Beard, Science **334**, 1530 (2011).

[43] A. Shabaev, Al. L. Efros, and A. J. Nozik, Nano Lett. **6**, 2856 (2006).

[44] H. Tahara, M. Sakamoto, T. Teranishi, and Y. Kanemitsu, Phys. Rev. Lett. **119**, 247401 (2017).

[45] P. Spinicelli, S. Buil, X. Quélin, B. Mahler, B. Dubertret, and J.-P. Hermier, Phys. Rev. Lett. **102**, 136801 (2009).

[46] P. P. Jha and P. Guyot-Sionnest, ACS Nano **3**, 1011 (2009).

[47] D. E. Gómez, J. van Embden, P. Mulvaney, M. J. Fernée, and H. Rubinsztein-Dunlop, ACS Nano **3**, 2281 (2009).

[48] Y.-S. Park, W. K. Bae, J. M. Pietryga, and V. I. Klimov, ACS Nano **8**, 7288 (2014).

[49] M. Nirmal, B. O. Dabbousi, M. G. Bawendi, J. J. Macklin, J. K. Trautman, T. D. Harris, and L. E. Brus, Nature **383**, 802 (1996).

[50] Al. L. Efros and M. Rosen, Phys. Rev. Lett. **78**, 1110 (1997).

[51] J. Zhao, G. Nair, B. R. Fisher, and M. G. Bawendi, Phys. Rev. Lett. **104**, 157403 (2010).

[52] S. Rosen, O. Schwartz, and D. Oron, Phys. Rev. Lett. **104**, 157404 (2010).

[53] C. Galland, Y. Ghosh, A. Steinbrück, M. Sykora, J. A. Hollingsworth, V. I. Klimov, and H. Htoon, Nature **479**, 203 (2011).

[54] C. Galland, Y. Ghosh, A. Steinbrück, J. A. Hollingsworth, H. Htoon, and V. I. Klimov, Nat. Commun. **3**, 908 (2012).

[55] Al. L. Efros and D. J. Nesbitt, Nat. Nanotechnol. **11**, 661 (2016).

[56] S. D. Stranks and H. J. Snaith, Nat. Nanotechnol. **10**, 391 (2015).

[57] B. R. Sutherland and E. H. Sargent, Nat. Photonics **10**, 295 (2016).

[58] Y. Kanemitsu, J. Mater. Chem. C **5**, 3427 (2017).

[59] K. Miyata, T. L. Atallah, and X.-Y. Zhu, Sci. Adv. **3**, e1701469 (2017).

[60] Y. Kanemitsu and T. Handa, Jpn. J. Appl. Phys., Part 1 **57**, 090101 (2018).

[61] M. V. Kovalenko, L. Protesescu, and M. I. Bodnarchuk, Science **358**, 745 (2017).

[62] Q. A. Akkerman, G. Rainò, M. V. Kovalenko, and L. Manna, Nat. Mater. **17**, 394 (2018).

[63] J.-P. Correa-Baena, M. Saliba, T. Buonassisi, M. Grätzel, A. Abate, W. Tress, and A. Hagfeldt, Science **358**, 739 (2017).

[64] T. Umebayashi, K. Asai, T. Kondo, and A. Nakao, Phys. Rev. B **67**, 155405 (2003).

[65] J. Even, L. Pedesseau, C. Katan, M. Kepenekian, J.-S. Lauret, D. Sapori, and E. Deleporte, J. Phys. Chem. C **119**, 10161 (2015).

[66] N. S. Makarov, S. Guo, O. Isaienko, W. Liu, I. Robel, and V. I. Klimov, Nano Lett. **16**, 2349 (2016).

[67] R. E. Brandt, J. R. Poindexter, P. Gorai, R. C. Kurchin, R. L. Z. Hoye, L. Nienhaus, M. W. B. Wilson, J. A. Polizzotti, R. Sereika, R. Žaltauskas, L. C. Lee, J. L. MacManus-Driscoll, M. Bawendi, V. Stevanović, and T. Buonassisi, Chem. Mater. **29**, 4667 (2017).

[68] T. Handa, H. Tahara, T. Aharen, and Y. Kanemitsu, Sci. Adv. **5**, eaax0786 (2019).

[69] M. Shirayama, H. Kadowaki, T. Miyadera, T. Sugita, M. Tamakoshi, M. Kato, T. Fujiseki, D. Murata, S. Hara, T. N. Murakami, S. Fujimoto, M. Chikamatsu, and H. Fujiwara, Phys. Rev. Appl. **5**, 014012 (2016).

[70] A. M. A. Leguy, P. Azarhoosh, M. I. Alonso, M. Campoy-Quiles, O. J. Weber, J. Yao, D. Bryant, M. T. Weller, J. Nelson, A. Walsh, M. van Schilfgaarde, and P. R. F. Barnes, Nanoscale **8**, 6317 (2016).

[71] Y. Yamada, T. Nakamura, M. Endo, A. Wakamiya, and Y. Kanemitsu, IEEE J. Photovoltaics **5**, 401 (2015).

[72] A. Miyata, A. Mitioglu, P. Plochocka, O. Portugall, J. T.-W. Wang, S. D. Stranks, H. J. Snaith, and R. J. Nicholas, Nat. Phys. **11**, 582 (2015).

[73] Y. Yamada, T. Nakamura, M. Endo, A. Wakamiya, and Y. Kanemitsu, J. Am. Chem. Soc. **136**, 11610 (2014).

[74] Y. Yamada, T. Yamada, L. Q. Phuong, N. Maruyama, H. Nishimura, A. Wakamiya, Y. Murata, and Y. Kanemitsu, J. Am. Chem. Soc. **137**, 10456 (2015).

[75] T. Yamada, T. Aharen, and Y. Kanemitsu, Phys. Rev. Lett. **120**, 057404 (2018).

[76] S.-T. Ha, C. Shen, J. Zhang, and Q. Xiong, Nat. Photonics **10**, 115 (2016).

[77] T. Yamada, T. Aharen, and Y. Kanemitsu, Phys. Rev. Mater. **3**, 024601 (2019).

[78] L. C. Schmidt, A. Pertegás, S. González-Carrero, O. Malinkiewicz, S. Agouram, G. M. Espallargas, H. J. Bolink, R. E. Galian, and J. Pérez-Prieto, J. Am. Chem. Soc. **136**, 850 (2014).

[79] L. Protesescu, S. Yakunin, M. I. Bodnarchuk, F. Krieg, R. Caputo, C. H. Hendon, R. X. Yang, A. Walsh, and M. V. Kovalenko, Nano Lett. **15**, 3692 (2015).

[80] G. Nedelcu, L. Protesescu, S. Yakunin, M. I. Bodnarchuk, M. J. Grotevent, and M. V. Kovalenko, Nano Lett. **15**, 5635 (2015).

[81] M. A. Becker, R. Vaxenburg, G. Nedelcu, P. C. Sercel, A. Shabaev, M. J. Mehl, J. G. Michopoulos, S. G. Lambrakos, N. Bernstein, J. L. Lyons, T. Stöferle, R. F. Mahrt, M. V. Kovalenko, D. J. Norris, G. Rainò, and Al. L. Efros, Nature **553**, 189 (2018).

[82] M. Nirmal, D. J. Norris, M. Kuno, M. G. Bawendi, Al. L. Efros, and M. Rosen, Phys. Rev. Lett. **75**, 3728 (1995).

[83] Al. L. Efros, M. Rosen, M. Kuno, M. Nirmal, D. J. Norris, and M. Bawendi, Phys. Rev. B **54**, 4843 (1996).

[84] G. Rainò, G. Nedelcu, L. Protesescu, M. I. Bodnarchuk, M. V. Kovalenko, R. F. Mahrt, and T. Stöferle, ACS Nano **10**, 2485 (2016).

[85] M. Fu, P. Tamarat, H. Huang, J. Even, A. L. Rogach, and B. Lounis, Nano Lett. **17**, 2895 (2017).

[86] M. Isarov, L. Z. Tan, M. I. Bodnarchuk, M. V. Kovalenko, A. M. Rappe, and E. Lifshitz, Nano Lett. **17**, 5020 (2017).

[87] C. Yin, L. Chen, N. Song, F. Lv, F. Hu, C. Sun, W. W. Yu, C. Zhang, X. Wang, Y. Zhang, and M. Xiao, Phys. Rev. Lett. **119**, 026401 (2017).

[88] D. Canneson, E. V. Shornikova, D. R. Yakovlev, T. Rogge, A. A. Mitioglu, M. V. Ballottin, P. C. M. Christianen, E. Lhuillier, M. Bayer, and L. Biadala, Nano Lett. **17**, 6177 (2017).

[89] L. Chen, B. Li, C. Zhang, X. Huang, X. Wang, and M. Xiao, Nano Lett. **18**, 2074 (2018).

[90] P. Tamarat, M. I. Bodnarchuk, J.-B. Trebbia, R. Erni, M. V. Kovalenko, J. Even, and B. Lounis, Nat. Mater. **18**, 717 (2019).

[91] J. A. Castañeda, G. Nagamine, E. Yassitepe, L. G. Bonato, O. Voznyy, S. Hoogland, A. F. Nogueira, E. H. Sargent, C. H. B. Cruz, and L. A. Padilha, ACS Nano **10**, 8603 (2016).

[92] M. Achermann, J. A. Hollingsworth, and V. I. Klimov, Phys. Rev. B **68**, 245302 (2003).

[93] G. Yumoto, H. Tahara, T. Kawawaki, M. Saruyama, R. Sato, T. Teranishi, and Y. Kanemitsu, J. Phys. Chem. Lett. **9**, 2222 (2018).

[94] N. Yarita, H. Tahara, T. Ihara, T. Kawawaki, R. Sato, M. Saruyama, T. Teranishi, and Y. Kanemitsu, J. Phys. Chem. Lett. **8**, 1413 (2017).

[95] G. Nair, J. Zhao, and M. G. Bawendi, Nano Lett. **11**, 1136 (2011).

[96] Y. S. Park, A. V. Malko, J. Vela, Y. Chen, Y. Ghosh, F. García-Santamaría, J. A. Hollingsworth, V. I. Klimov, and H. Htoon, Phys. Rev. Lett. **106**, 187401 (2011).

[97] J. Zhao, O. Chen, D. B. Strasfeld, and M. G. Bawendi, Nano Lett. **12**, 4477 (2012).

[98] N. Hiroshige, T. Ihara, and Y. Kanemitsu, Phys. Rev. B **95**, 245307 (2017).

[99] N. Hiroshige, T. Ihara, M. Saruyama, T. Teranishi, and Y. Kanemitsu, J. Phys. Chem. Lett. **8**, 1961 (2017).

[100] G. Yuan, C. Ritchie, M. Ritter, S. Murphy, D. E. Gómez, and P. Mulvaney, J. Phys. Chem. C **122**, 13407 (2018).

[101] G. Rainò, A. Landuyt, F. Krieg, C. Bernasconi, S. T. Ochsenbein, D. N. Dirin, M. I. Bodnarchuk, and M. V. Kovalenko, Nano Lett. **19**, 3648 (2019).

[102] N. Yarita, H. Tahara, M. Saruyama, T. Kawawaki, R. Sato, T. Teranishi, and Y. Kanemitsu, J. Phys. Chem. Lett. **8**, 6041 (2017).

[103] B. A. Koscher, J. K. Swabeck, N. D. Bronstein, and A. P. Alivisatos, J. Am. Chem. Soc. **139**, 6566 (2017).

[104] M. I. Bodnarchuk, S. C. Boehme, S. ten Brinck, C. Bernasconi, Y. Shynkarenko, F. Krieg, R. Widmer, B. Aeschlimann, D. Günther, M. V. Kovalenko, and I. Infante, ACS Energy Lett. **4**, 63 (2019).

[105] D. P. Nenon, K. Pressler, J. Kang, B. A. Koscher, J. H. Olshansky, W. T. Osowiecki, M. A. Koc, L.-W. Wang, and A. P. Alivisatos, J. Am. Chem. Soc. **140**, 17760 (2018).

[106] J. D. Rinehart, A. M. Schimpf, A. L. Weaver, A. W. Cohn, and D. R. Gamelin, J. Am. Chem. Soc. **135**, 18782 (2013).

[107] K. Wu, J. Lim, and V. I. Klimov, ACS Nano **11**, 8437 (2017).

[108] R. Matsunaga, K. Matsuda, and Y. Kanemitsu, Phys. Rev. Lett. **106**, 037404 (2011).

[109] S. M. Santos, B. Yuma, S. Berciaud, J. Shaver, M. Gallart, P. Gilliot, L. Cognet, and B. Lounis, Phys. Rev. Lett. **107**, 187401 (2011).

[110] T. Nishihara, Y. Yamada, and Y. Kanemitsu, Phys. Rev. B **86**, 075449 (2012).

[111] N. Yarita, T. Aharen, H. Tahara, M. Saruyama, T. Kawawaki, R. Sato, T. Teranishi, and Y. Kanemitsu, Phys. Rev. Mater. **2**, 116003 (2018).

[112] S. Ye, W. Sun, Y. Li, W. Yan, H. Peng, Z. Bian, Z. Liu, and C. Huang, Nano Lett. **15**, 3723 (2015).

[113] J. A. McGuire, J. Joo, J. M. Pietryga, R. D. Schaller, and V. I. Klimov, Acc. Chem. Res. **41**, 1810 (2008).

[114] S. Nakahara, H. Tahara, G. Yumoto, T. Kawawaki, M. Saruyama, R. Sato, T. Teranishi, and Y. Kanemitsu, J. Phys. Chem. C **122**, 22188 (2018).

[115] S. Nakahara, K. Ohara, H. Tahara, G. Yumoto, T. Kawawaki, M. Saruyama, R. Sato, T. Teranishi, and Y. Kanemitsu, J. Phys. Chem. Lett. **10**, 4731 (2019).

[116] H.-C. Wang, W. Wang, A.-C. Tang, H.-Y. Tsai, Z. Bao, T. Ihara, N. Yarita, H. Tahara, Y. Kanemitsu, S. Chen, and R.-S. Liu, Angew. Chem., Int. Ed. **56**, 13650 (2017).

[117] K. Ohara, T. Yamada, H. Tahara, T. Aharen, H. Hirori, H. Suzuura, and Y. Kanemitsu, "Excitonic enhancement of optical nonlinearities in perovskite CH3NH3PbCl3 single crystals," Phys. Rev. Mater. (in press).

[118] G. Rainò, M. A. Becker, M. I. Bodnarchuk, R. F. Mahrt, M. V. Kovalenko, and T. Stöferle, Nature **563**, 671 (2018).

[119] K. Wu, Y.-S. Park, J. Lim, and V. I. Klimov, Nat. Nanotechnol. **12**, 1140 (2017).

[120] Y. Wang, M. Zhi, Y.-Q. Chang, J.-P. Zhang, and Y. Chan, Nano Lett. **18**, 4976 (2018).

[121] T. Handa, A. Wakamiya, and Y. Kanemitsu, APL Mater. **7**, 080903 (2019).

[122] M. D. Smith and H. I. Karunadasa, Acc. Chem. Res. **51**, 619 (2018).

[123] B. M. Benin, D. N. Dirin, V. Morad, M. Wörle, S. Yakunin, G. Rainò, O. Nazarenko, M. Fischer, I. Infante, and M. V. Kovalenko, Angew. Chem. **130**, 11499 (2018).

[124] T. Jun, K. Sim, S. Iimura, M. Sasase, H. Kamioka, J. Kim, and H. Hosono, Adv. Mater. **30**, 1804547 (2018).

[125] J. Luo, X. Wang, S. Li, J. Liu, Y. Guo, G. Niu, L. Yao, Y. Fu, L. Gao, Q. Dong, C. Zhao, M. Leng, F. Ma, W. Liang, L. Wang, S. Jin, J. Han, L. Zhang, J. Etheridge, J. Wang, Y. Yan, E. H. Sargent, and J. Tang, Nature **563**, 541 (2018).